International Congress of Science and Technology of Metallurgy and Materials, SAM - CONAMET 2013

Forming Limit Curve Determination of a DP-780 Steel Sheet

Claudio D. Schwindt[a]*, Mike Stout[b], Lucio Iurman[a], Javier W. Signorelli[b]

[a] *Grupo de Metalurgia y Tecnología Mecánica, UNS-CONICET, Av. Alem 1253 - Bahía Blanca (8000), Argentina.*
[b]*Grupo de Física y Micromecánica de Materiales Heterogéneos, IFIR-UNR-CONICET, Bv. 27 de Febrero 210b, Rosario (S2000BTP), Santa Fe, Argentina.*

Abstract

In the present work, the forming limit curve (FLC) of a 1.1 mm thick DP-780 steel sheet is evaluated. The full FLC determination involved tensile tests of planar samples with different notch geometries – providing data in the tension-compression range – and Nakajima tests with a 40 mm diameter hemispherical punch and different notch geometries, covering the full loading zone of the forming limit diagram. The proposed Nakajima tool geometry reduces the standard test dimensions (ISO 12004-2) by 60%. Results show that the reduced diameter Nakajima test, in the particular case of Dual-Phase steels, overestimates limit strains when compared to the tensile test. This observed difference is explained in terms of the presence of a strain gradient through the sheet thickness imposed by the 40 mm diameter Nakajima punch, leading to the conclusion that this reduced sample type is not suitable for FLC determination when the DP-780 steel sheet is more than a millimeter thick.

1. Introduction

   Along with the intensification of the global energetic crisis and environmental issues, energy saving and car safety have become a major priority for the automotive industry. One of the strategies adopted is to replace conventional steels in car bodies with Advanced High Strength Steels (AHSS), thus achieving significant weight

   * Corresponding author. Tel.: +54-0291-4595179.
      E-mail address: claudio.schwindt@uns.edu.ar

reduction, lower fuel consumption, as well as reduced pollution emissions (Sperle and Olsson, 1994; Lee et al., 2010).

Conventional High Strength Steels (HSS) are hardened by solid-solution precipitation or grain refinement. In contrast, phase transformations are the main hardening processes for AHSS, which are defined according to their microstructural features and the combination of different phases. The observed microstructures may include ferrite, martensite, bainite and retained austenite. Dual-phase (DP), transformation-induced plasticity (TRIP), complex-phase (CP), and martensitic (MART) steels are some of the grades collectively referred to as AHSS. Compared with conventional HSS, these steels are superior in combining strength and ductility, and thus they facilitate energy absorption during impact, which improves crash performance and the assurance of safety, while reducing weight (Senuma, 2001; Heller et al., 1998).

DP steels belong to the AHSS group, and their increasing application is due to their excellent combination of mechanical properties such as high tensile strength, high work-hardening rate and very good ductility. Knowledge of the formability behavior of these sheet metals is critical for the success of stamping operations in the automotive industry. In order to determine the critical strain states that limit formability, Keeler and Backofen (1963) and Goodwin (1968) developed a graphical tool called the forming limit diagram (FLD), which is currently widely used in the metalworking industry. The FLD captures the principal-strain values experienced by surface elements of sheet metals subjected to formability tests along different strain-paths under plane-stress conditions. In this way, it allows the establishment of a boundary between two zones: a safe area, where the risk of necking or excessive thinning is negligible, and an unsafe area, in which such instability can take place. The boundary between these two zones is usually a line drawn manually from the measured strain values in forming limit specimens. This line is called the forming limit curve (FLC).

In the present work, the FLC of a 1.1 mm thick DP-780 steel sheet is evaluated. The experimental procedure involved tensile tests of planar samples with different notch geometries – providing data in the tension-compression range – and Nakajima tests with a 40 mm diameter hemispherical punch and different notch geometries in the full FLC determination. The proposed Nakajima tool geometry reduces the standard test dimensions (ISO 12004-2) by 60%. Results show that the reduced diameter Nakajima test, in the particular case of Dual-Phase steels, overestimates limit strains when compared to the tensile test. This observed difference is explained in terms of the presence of a strain gradient through the sheet thickness imposed by the 40 mm diameter Nakajima punch, leading to the conclusion that this reduced sample type is not suitable for FLC determination when the DP-780 steel sheet is more than a millimeter thick.

2. Experimental work

2.1. Material

In the present work, we considered a 1.1 mm thick dual-phase steel sheet, having a tensile strength of 780 MPa (DP-780). The chemical composition of the material is given in Table 1.

Table 1. Chemical composition of the steel sheet.

Element	C	Si	Mn	P	S	Cr	Ni	Mo	Al	Ti
Wt. %	0,16	0,235	1,95	0,022	0,007	0,32	0,024	0,105	0,132	0,027

The material's microstructure was characterized using a Leica DM ILM optical microscope. The micrographs (Fig. 1 (left) and Fig. 1 (right)) show a ferritic/martensitic microstructure with the martensite appearing as irregular bands along the rolling direction. We found a martensitic volume fraction of 30%. The samples were prepared by conventional metallographic techniques using the LePera reactant (LePera, 1979) to reveal the martensite and ferrite phases in white and brown colors respectively. The martensite volume fraction was determined by means of the image analysis software Leica Application Suite v4.0.
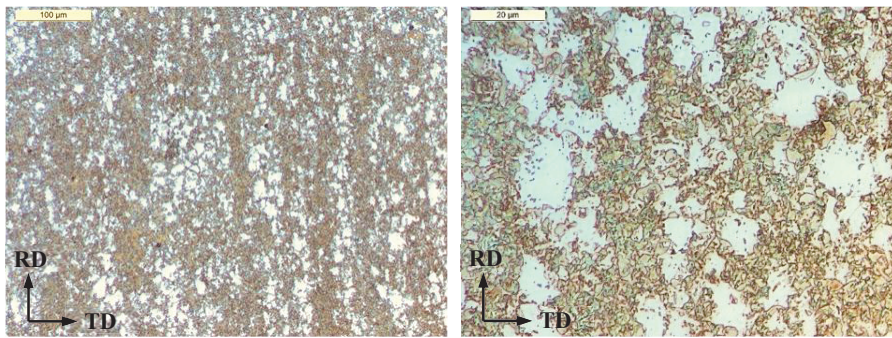
Fig. 1. Optical micrographs of the DP-780 steel: (left) 200x; (right) 1000x.

Texture measurements were conducted using X-ray diffraction in a Phillips X'Pert Pro-MPD system equipped with a texture goniometer, Cu Kα radiation and an X-ray lens. The initial pole figures obtained for the {110}, {112} and {100} diffraction peaks are shown in Fig. 2 (left). From these data, following Van Houtte's methodology (Van Houtte, 1995), the orientation distribution function (ODF) was calculated. The measured texture represented by the $\varphi_2=45°$ section is also plotted in Fig. 2 (right). It shows a typical cold-rolled and annealed steel texture with low intensities.
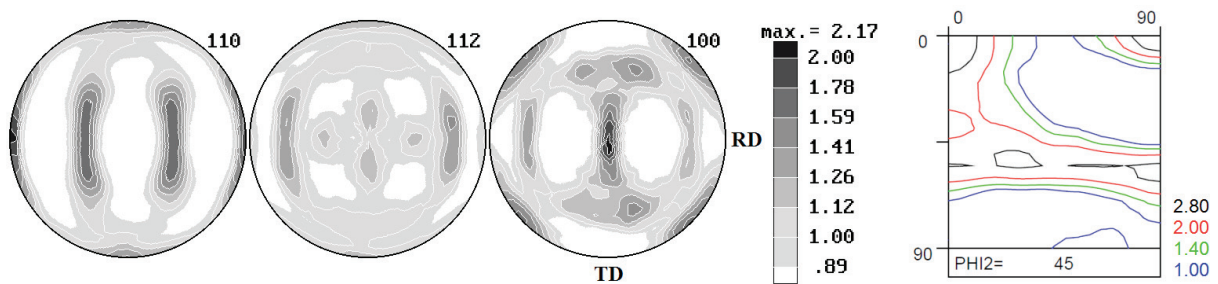

Fig. 2. Experimental equal-area pole figures {110}, {112} and {100} (left); $\varphi_2=45°$ section of the ODF (right).

The mechanical properties of the material were obtained following the ASTM E8M standard on planar subsize specimens along the rolling direction (RD), the diagonal direction (DD) and the transverse direction (TD), i.e., at 0°, 45° and 90° to the rolling direction. Duplicated samples were tested and the results were averaged in each direction. The usual strain-hardening parameters corresponding to Hollomon's law were obtained from fitting the uniaxial true-stress/true-strain curve between 5 and 12 percent true strain for each of the three tensile-sample orientations. The R-values were determined from measurements of longitudinal and transverse strains and the assumption of constancy of volume. These measurements were made with additional tensile specimens stretched to 10% engineering strain. The basic material properties of the DP-780 steel are listed in Table 2. All experimental tests were conducted at room temperature.

Table 2. Mechanical properties of the material.

Sample orientation	$\sigma_{0,2}$ (MPa)	σ_T (MPa)	A%	K (MPa)	n	$R_{10\%}$
Longitudinal (RD)	507	832,5	12,5	1240	0,131	0,74
Diagonal (DD)	501,5	821,5	12,7	1235	0,135	1,00
Transversal (TD)	498,5	844	12,3	1263	0,133	0,87
Mean value	502,1	829,9	12,5	1243	0,134	0,90

Tensile specimens were loaded in displacement control at a crosshead speed of 1.5 mm/min, using a 100 kN capacity Instron 3382 Universal Testing System. This displacement rate gave a strain rate of about 10^{-3} s^{-1}. The measured loading curves for the uniaxial tensile tests are plotted in Fig. 3.
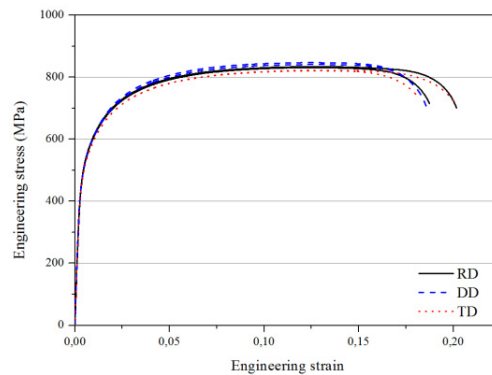

Fig. 3. The measured engineering stress-strain curves in uniaxial tension.

2.2. Forming limit curve determination

Due to the complex nature of industrial sheet-metal forming processes, a large amount of tests is needed to assess formability under different deformation conditions. In the present work, the experimental determination of the FLC was carried out by two tests: tensile tests of notched planar specimens, providing data in the tension-compression range; and Nakajima tests with a hemispherical punch, which gives data over the full range of deformation. Both types of tests were conducted using a 100 kN capacity Instron 3382 Universal Testing System.

Four tensile sample geometries were used in order to achieve different sheet deformation conditions, from simple uniaxial-tension to plane-strain deformation states (Fig. 4 (left)). All specimens were oriented with their principal axis along the rolling direction. The specimens' dimensions are shown in Fig. 4 (right). Two samples per geometry were tested and the crosshead speed of the testing machine was 0.5, 0.4, 0.2 and 0.1 mm/min for the geometries 1 to 4 respectively. The results are presented in Fig. 8 (left).
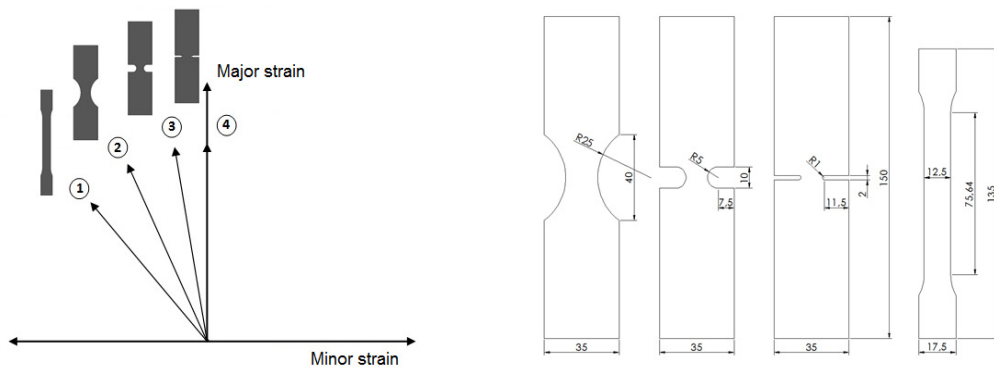

Fig. 4. Different types of specimen representative of the linear strain paths (left); samples dimensions (right)

The Nakajima test is the most common method for determining the FLC of sheet metals. The test is based on deforming specimens with different geometries up to fracture using a hemispherical punch. Fig. 5 shows the punch and die set used. The proposed Nakajima tool geometry reduces the standard test dimensions (ISO 12004-2) by 60%, and achieves states between uniaxial-tension and balanced-biaxial deformation, by varying the width of the

hourglass-shaped samples shown in Fig. 5 (W = 20 mm, 40 mm, 50 mm, 55 mm, 60 mm, 70 mm, 80 mm). The specimens were mounted with their gridded side opposite to the 40 mm diameter hemispherical punch and stretched with a punch velocity of 0.5 mm/min up to a noticeable drop in the load, which indicates the start of localized necking.
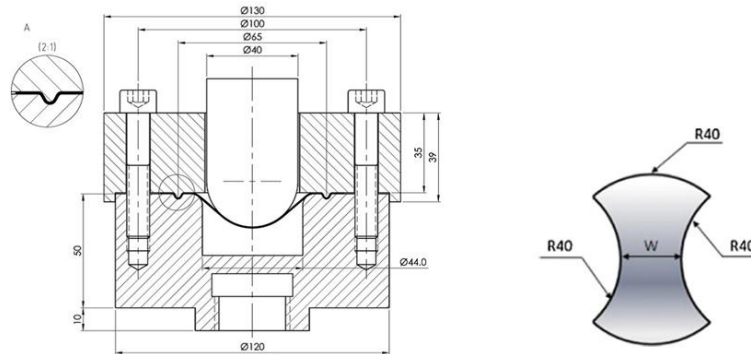

Fig. 5. The punch, die and die cap used for measuring the FLD (left); specimen geometry used in experimental work (right).

Two specimens of each blank width, oriented with their principal axis in the rolling direction, were tested to get a sufficient number of data points. A thin layer of MoS_2-based lubricant was aerosol painted on the specimen surface facing the punch, to produce adequate lubrication conditions. A 0.2 mm thick sheet of polytetrafluorethylene film was used to provide additional lubrication for all hourglass samples. In the case of the biaxial specimens (W=80mm), a 4 mm thick disk of polyurethane 40 mm in diameter was used for lubrication. The FLC obtained is shown in Fig. 8 (right).

2.3. Strain measurements

In the tensile tests, the strains were measured with the Digital Image Correlation (DIC) technique (Sutton et al. 2009). This is a non-invasive method that allows for full displacement-field determination on the surface of the specimen, by analysis of digital images taken during testing. Depending on whether the displacement occurs in the plane or out of it, the DIC technique should be used in two or three dimensions. In order to use this method, samples are artificially speckled by applying fine black aerosol-paint spots on a painted white surface. This leads to a highly contrasted image of randomly disposed points (Fig. 6).
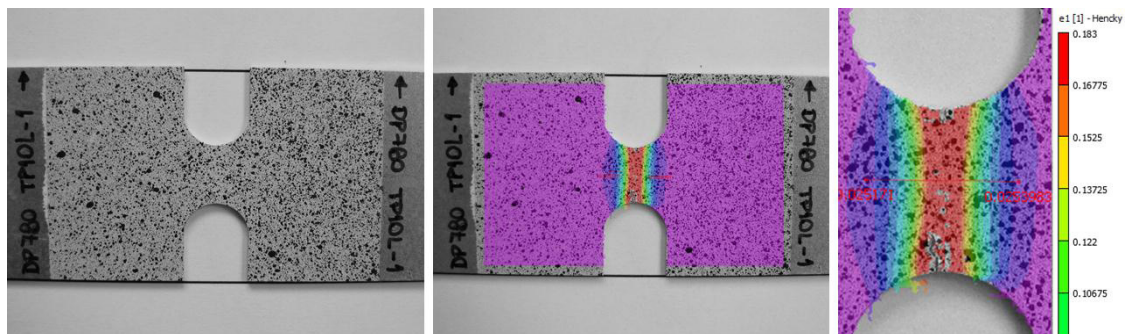

Fig. 6. Application of DIC technique on tensile specimens: speckle pattern (left); major Hencky strain (center); detail (right)

After the strain field is known from the image correlation analysis, a methodology must be selected in order to determine the critical-strain values. Different FLCs can be obtained for the same material using different

measurement criteria and/or experimental methods. Therefore, the establishment of a reference method or technique to determine the FLC is still an issue in sheet metal forming. Several experimental methods have been proposed for this purpose (NF EN ISO 12004-2 2008, Sene et al. 2008, Matin et al. 2006, Makkouk et al. 2008, Puccinelli et al. 2011, Bragard et al. 1972). However, only the Bragard method (Bragard et al. 1972) was used in the present work. This technique is based on the analysis of a blank with necking or fracture present. Once the full strain field is determined, the maximum principal strain is extracted along a section normal to the fracture. After conveniently discarding a zone around the fracture, the limit-strain value is found by fitting a polynomial function through the remaining strain points. The polynomial's maximum lies in the region of the discarded fracture-zone data and it is an interpolation between the two remaining data sets. This maximum is considered to be the critical major-strain value and it is thus one point of the FLC.

The strains obtained in Nakajima specimens were measured with the conventional circle-grid method, using a pattern of non-contacting 2.50 mm diameter circles electrochemically deposited on the samples. After testing, major and minor dimensions of the deformed circles (ellipses), with uniform, localized and fracture deformations, were measured with a combination low power microscope (20X) and digital camera. The digital camera's associated image acquisition and editing software gave the actual circle dimension. Due to the large dispersion involved with this measurement method, it is difficult to determine a precise curve that delineates the beginning of localized necking. Consequently, it is more appropriate to show a band instead of a line on the FLD.
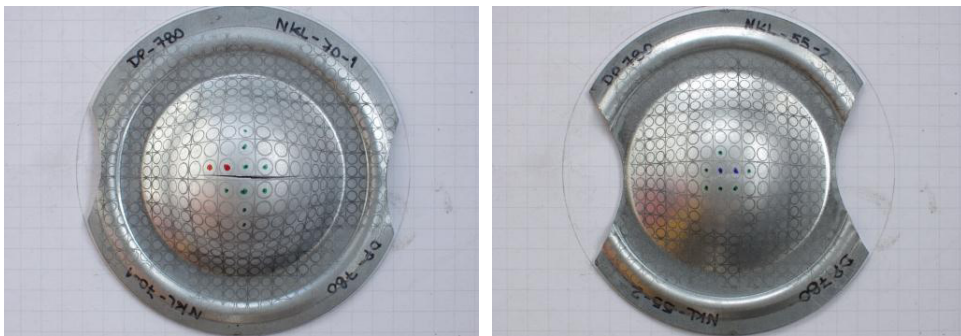

Fig. 7. Grid pattern of circles printed on the surface of the Nakajima samples

3. Results and discussions

The experimental FLCs are shown in Fig. 8. The maximum principal strains are plotted along the y-axis and the minimum principal strain along the x-axis. Open, grey and black circles correspond to uniform deformation, localized necking and fracture data, respectively. The transition between uniform deformation and localized necking and fracture defines a boundary between a safe and insecure deformation for metal forming (dashed line). The minimum limit-strain value occurs near the plane-strain condition ($\rho=\varepsilon_2/\varepsilon_1=0$), with $\varepsilon_{1min}=0.15$, while the maximum values were measured for strain paths between $\rho=0.4$ and $\rho=0.7$. The balanced-biaxial stretching values were slightly lower than the maximum. This can be explained in terms of the curvature of the yield surface (Serenelli et al. 2010).

The use of different notched geometries in the tensile tests allowed us to obtain the full left-hand side of the FLC. Results show a clear boundary between zones of homogeneous and necking or fracture deformation, which facilitates the drawing of the forming-limit curve (Fig. 8 left). On the other hand, the FLC determination with Nakajima tests has a greater uncertainty due to the large dispersion in the data produced by the gridding technique (Fig. 8 right). Nakajima samples with the complete circular geometry approached balanced-biaxial deformation, while intermediate widths of 40 and 50 mm give nearly plane-strain deformation. The narrowest sample (W=20mm) tended towards a uniaxial-tension deformation state. An inspection over the complete experimental FLD shows that the minimum values of unsafe deformations do not lie on the plane-strain axis ($\varepsilon_2 = 0$) but are systematically shifted to the right-hand side of the diagram. This shift is related to the intrinsic strain path non-linearity induced by the

hemispheric Nakajima punch. The punch imposes an equi-biaxial strain state at the beginning of the test, which changes gradually to the intended path (given by the sample geometry and material properties) only after a finite amount of deformation.
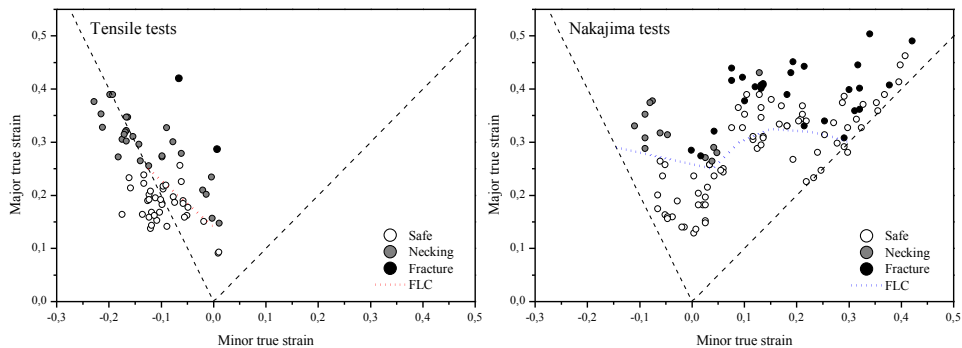

Fig. 8. Experimental FLDs of the DP-780 steel sheet by tensile tests (left) and Nakajima tests (right)

Results show that the reduced diameter Nakajima test overestimates limit strains – Fig 8 (right) – by as much as 70% (plane-strain deformation) as compared to the tensile test, when the notched specimens producing strain states on the left-hand side of the FLD are considered – Fig. 8 (left). This observed increase in formability is explained in terms of the presence of a strain gradient through the sheet thickness caused by the superposition of stretch-bending imposed by the punch and die geometry inherent in the Nakajima test. This phenomenon, first addressed by Ghosh and Hecker, 1974; delays strain localization, allowing for higher levels of deformation before failure. Shi and Gerdeen, 1991 introduced the effect of curvature in the MK analysis modifying the constitutive equation to include a gradient term. The results showed that an increase in curvature causes an increase in the limit strain. Consequently, a higher level of deformation is expected from the Nakajima test, than that obtained with planar specimens (no curvature effects). This effect can be observed in conventional steels, but it is much more pronounced in AHSS steels (Till et al. 2008). These materials exhibit a high hardening rate in the first stages of deformation compared to conventional steels, which would retard the onset of necking. Even though we have not verified in the current study, it is expected that the presence of a strain gradient similarly affects the right-hand side of the FLC. We are currently working to get planar specimen geometries in order to perform Marciniak tests that cover this side of the FLD, and thus, we will be able to observe the influence of the strain gradient through the sheet thickness over the whole range of deformation. The Marciniak test has the advantage of deforming a flat area in the center of the specimen that has not undergone bending or friction with the punch. In addition, if necking or fracture occurs on a flat surface, only a 2D image-correlation analysis with a single camera is required.

4. Conclusions

In the present work, the forming limit curve for a 1.1 mm thick DP-780 steel sheet was evaluated using two tests: tensile tests with notched specimens; and Nakajima tests with different sample geometries. In the case of the notched tensile specimens, data on the left-hand side of the FLD is obtained using digital image correlation and a Bragard type analysis. The digital image correlation technique saves time and increases the strain-measurement accuracy. The Nakajima test allowed for the determination of the complete FLD by varying only the samples' width. However, the reduced punch and die set dimensions with respect to the standard test dimensions resulted in abnormally high limit strains, mainly in a plane-strain condition. Thus, the reduced specimen geometry can overestimate the FLC of this material. This observed difference is explained in terms of the presence of a strain gradient through the sheet thickness. The gradient is imposed by the 40 mm diameter Nakajima punch, leading to the conclusion that this reduced sample type is not suitable for FLC determination when the DP-780 steel sheet is more than a millimeter thick.

Acknowledgements

The authors would like to thank R. Bruna for his significant contribution to the experimental work and Nibbler Company (Rosario, Santa Fe Province, Argentina) for their collaboration in the preparation of samples.

References

Bragard, A., Baret, J.C., Bonnarens, H, 1972. A simplified technique to determine FLD at the onset off necking. Rapport du Centre de Recherchers Mettallurgiques, No. 33.

Goodwin, G.M., 1968. Application of strain analysis to sheet metal forming problems in the press shop. La Metallurgia Italiana 8, 767-774.

Ghosh, A.K., Hecker, S.S., 1974. Stretching limits in sheet metals: In-plane versus out-of-plane deformation. Metallurgical Transactions 5, 2161-2164.

Heller, T., End, B., Ehrhardt, B., irgenEsdohr, J., 1998. New High Strength Steels Production, Properties & Applications. Proc. of 40th ISS Mechanical Working and Steel Processing (MWSP) Conference, 25-34.

Keeler, S.P., Backofen, W.A., 1963. Plastic instability and fracture in sheets stretched over rigid punches. ASM Transactions 56, 25-48.

Lee, H.W., Kim, G., Park, S.H., 2010. Lightweight Steel Solutions for Automotive Industry. NUMIFORM, Proceedings of the 10th International Conference, 55-62.

Lepera, F.S., 1979. Improved Etching Techniques for the Determination of Percent Martensite in High-strength Dual-Phase Steel. Metallography 12, 79-81.

Makkouk, R., Bourgeois, N., Serri, J., Bolle, B., Martiny, M., Teaca, M., Ferron, G., 2008. Experimental and theoretical analysis of the limits to ductility of type 304 stainless steel sheet. European Journal of Mechanics A/Solids 27, 181-194.

Matin, P.H., Smith, L.M., Petrusevski, S., 2006. A method for stress space forming limit diagram construction for aluminum alloys. Journal of Materials Processing Technology 174, 258-265.

NF EN ISO 12004-2:2008-12 European Standard. Metallic materials Sheet and strip. Determination of forming-limit curves. ISSN 0335-3931.

Puccinelli, M., Schwindt, C., Serenelli, M., Signorelli, J., 2011. Evaluación de dos métodos para la determinación experimental del límite de conformado equibiaxial. Anales SAM / CONAMET, 1-6.

Sène, N.A., Balland P., Arrieux, R., 2008. About necking detection to determine forming limit diagrams for mini stamping. 17th International Science and Technology Conference, 241-253.

Senuma, T., 2001. Physical Metallurgy of Modern High Strength Steel Sheets, ISIJ International 41, 520-532.

Serenelli, M., Bertinetti, M.A., Signorelli, J.W., 2010. Investigation of the dislocation slip assumption on formability of BCC sheet metals"; International Journal of Mechanical Sciences 52, 1723–1734.

Shi, M.F., Gerdeen, J.C., 1991. Effect of strain gradient and curvature on Forming Limit Diagrams for Anisotropic Sheets. J. Materials Shaping Technology 9, 253-268.

Sperle, J.O., Olsson, K., 1994. High-Strength Automotive Sheet Steels for Weight Reduction and Safety Applications. High-Strength Steels for Automotive Symposium Proceedings, 65-77.

Sutton, M.A., Orteu, J.-J., Schreier, H.W., 2009. Image Correlation for Shape, Motion and Deformation Measurements. Springer Publishing Company, Incorporated.

Till, E.T., Berger, E., Larour, P., 2008. On an Exceptional Forming Behaviour Aspect of AHSS Sheets. Proceedings of IDDRG, 429-440.

Van Houtte, P., 1995. Manual of the MTM-FHM software, Department MTM, K.U. Leuven.